

# INVISIBLE INFECTIONS: A PARTIAL INFORMATION APPROACH FOR ESTIMATING THE TRANSMISSION DYNAMICS OF THE COVID-19 PANDEMIC

KATIA COLANERI, CAMILLA DAMIAN, AND RÜDIGER FREY

**ABSTRACT.** In this paper, we develop a discrete time stochastic model under partial information to explain the evolution of Covid-19 pandemic. Our model is a modification of the well-known SIR model for epidemics, which accounts for some peculiar features of Covid-19. In particular, we work with a random transmission rate and we assume that the true number of infectious people at any observation time is random and not directly observable, to account for asymptomatic and non-tested people. We elaborate a nested particle filtering approach to estimate the reproduction rate and the model parameters. We apply our methodology to Austrian Covid-19 infection data in the period from May 2020 to June 2022. Finally, we discuss forecasts and model tests.

**Keywords:** stochastic SIR model, Covid-19, nested particle filtering, parameter inference, partially observable Markov processes.

## 1. INTRODUCTION

The Covid-19 pandemic renewed the interest in epidemiological models for the transmission of infectious diseases. In the last few years, research on this topics has grown substantially and classical models have been extended in order to better explain and predict the spreading of the virus. A large part of this literature is based on variants of the classical SIR model. The basic SIR model is a *compartmental* model, where the population is divided in three categories: the susceptible (individuals who can get infected); the infectious (individuals who spread the disease); the removed (individuals who cannot get infected, essentially since they enjoy immunity). The number of susceptible, infectious and removed individuals at time  $t$  is denoted by  $S_t$ ,  $I_t$  and  $R_t$ . The quantities  $(S, I, R)$  form the state variables of a SIR model. In the original formulation, the dynamics of state variables are deterministic and described by a system of ordinary differential equations (in continuous time) or difference equations (in discrete time).

In this paper, we propose several extensions of the classical SIR model that account for significant features of Covid-19. First, Covid-19 infections have to be confirmed by a medical test and many infections are not detected (invisible infections), since they are, for instance, asymptomatic or since

---

KATIA COLANERI, DEPARTMENT OF ECONOMICS AND FINANCE, UNIVERSITY OF ROME TOR VERGATA, VIA COLUMBIA 2, 00133 ROME, ITALY.

CAMILLA DAMIAN, INSTITUTE OF STATISTICS AND MATHEMATICAL METHODS IN ECONOMICS, TU WIEN, WIEDNER HAUPTSTR. 7, 1040 VIENNA, AUSTRIA

RÜDIGER FREY, INSTITUTE FOR STATISTICS AND MATHEMATICS, VIENNA UNIVERSITY OF ECONOMICS AND BUSINESS, WELTHANDELPATZ 1, 1020 VIENNA, AUSTRIA

*E-mail addresses:* [katia.colaneri@uniroma2.it](mailto:katia.colaneri@uniroma2.it), [camilla.damian@tuwien.ac.at](mailto:camilla.damian@tuwien.ac.at), [rfrey@wu.ac.at](mailto:rfrey@wu.ac.at).

We are grateful to Sylvia Frühwirth-Schnatter and Luca Gonzato for useful comments and suggestions.

infected individuals do not take a test. This implies that  $I_t$  is not directly observable; instead, the analyst observes only the time series of newly reported positive tests. Moreover, positively tested people are subject to quarantine measures and are therefore removed from the pool of infectious people, which affects the dynamics of the epidemic. Second, the infection or transmission rate  $\beta_t$  (i.e. the rate at which a susceptible individual gets infected given the number of infectious people at time  $t$ ) is influenced by many random factors such as policy measures, environmental conditions or changes in the infectivity of the virus, so that this quantity should be modelled as a stochastic process. Third, there is some randomness in the transmission process of the epidemic, in particular if the population size is small. We therefore model the state variables  $S, I, R$  and  $\beta$  as a discrete-time Markov process with transition probabilities mimicking the standard SIR-dynamics and where the infection rate is modelled as the exponential of some autoregressive process.

While natural from an epidemiological viewpoint, these extensions make statistical inference for our model a challenging task. Since  $I$  and  $\beta$  are not directly observable, we face an inference problem under partial information whose likelihood function is intractable. To overcome this issue we resort to a Bayesian approach based on sophisticated techniques from stochastic filtering. More precisely, we adapt the nested particle filter of Crisan and Miguez (2018) to our setup and compute approximations of the conditional distribution of the state variables and of the model parameters, given the observed series of positive tests. Simulation experiments demonstrate the good performance and the robustness of this methodology. We further apply the model to Covid-19 infection data from Austria. A comparison with official estimates from the Austrian health agency AGES shows that our model produces qualitatively similar results for the *effective reproduction number*. The latter is a measure for the number of individuals that are, on average, infected by an infectious person, given the state of the pandemic system. This confirms that our partial information model can be calibrated to real Covid-19 infection data. An important application of epidemiologic models is the forecasting of future infection numbers; these forecasts are used to gauge potential stress for the health system and to inform decisions on containment measures. In a Bayesian context - such as ours - forecasts are based on the *predictive distribution*, so that parameter uncertainty is taken into account naturally. We use simulations to compute the predictive distribution for the Austrian data and we study its properties. Moreover, we propose formal goodness of fit tests for the predictive distribution. An application of these tests to the Austrian infection data supports our methodology. Summarizing, our results show that statistical inference for an elaborated epidemiological model with partial information is indeed feasible, if one uses using advanced tools from stochastic filtering.

We continue with a discussion of the relevant literature. While the literature on SIR models is large, there are, to the best of our knowledge, only few contributions that treat statistical inference for epidemiological models as an estimation problem under partial information. Hasan et al. (2022) use the extended Kalman filter (EKF) in an SIR model with added Gaussian noise to analyse Scandinavian Covid-19 data. However, their model dynamics are somewhat implausible; in particular, the effective reproduction number is modelled as a random walk with Gaussian increments and can therefore become negative. Moreover, the SIR model is a nonlinear system and the EKF has to linearize these dynamics in a somewhat ad-hoc fashion, so that optimality and stability of the EKF cannot be guaranteed (see, e.g. Budhiraja et al. (2007)). On the other hand, the EKF is comparatively simple and it often works well when nonlinearities are small.

Stocks et al. (2020) study a partial information model for the dynamics of Rotavirus infections in Germany. Their model has structural similarities to ours; the details however differ substantially, since Stocks et al. (2020) study another type of virus and, most importantly, they use a different model for the dynamics of the infection rate. Moreover, the approach to partial information is not the same as ours, as they use a frequentist estimation methodology and compute the MLE for the model parameters via the *iterated filtering* approach of Ionides et al. (2015), whereas we rely on particle filtering to determine the posterior distribution of the model parameters in a Bayesian spirit. A few other interesting papers are Sun et al. (2015) and Alòs et al. (2021). Sun et al. (2015) represents another relevant contribution to Bayesian methods for parameter estimation. This paper provides a comparison study of three dynamical models for the evolution of biological, ecological or environmental processes. Namely it studies a deterministic model, a Markov-chain based model and a model described by stochastic differential equations showing the advantages and disadvantages of using one model or another. In Alòs et al. (2021), the authors propose an extension of the SIR model where infections are fully observable and where the infection rate  $\beta_t$  is assumed to follow a fractional Brownian motion. Their model seems to capture quite well the *observed* number of infection of Italian Covid-19 data during the very early period of the pandemic.

The rest of the paper is organized as follows. In Section 2 we introduce the setup; in Sections 3 and 4 we describe the nested particle filter and we present results for simulated data; Section 5 is concerned with applications to Austrian infection data and in Section 6 we discuss forecasts and model tests.

## 2. MODEL SPECIFICATION

In the sequel we introduce a stochastic version of the classical SIR model from epidemics, which accounts for the fact that the number of infected people as well as the infection rate are not observable.

*State variables and dynamics.* We work in a discrete time setting with time points  $t_n$ ,  $n = 0, 1, \dots$ , where  $t_n - t_{n-1}$  is one day. We consider a population with  $N$  individuals and we assume, for simplicity, that the population size stays constant (in particular, we ignore deaths caused by the pandemic). We introduce some notation. Let

- $S_n$  be the number of susceptible individuals at time  $t_n$ ;
- $I_n$  be the number of infectious persons at time  $t_n$  who can generate new infections in the period  $[t_n, t_{n+1})$ ;
- $I_n^+$  be the number of individuals who get infected in  $[t_{n-1}, t_n)$ ;
- $P_n$  be the number of positive tests in the interval  $[t_{n-1}, t_n)$ ;
- $I_n^-$  be the number of individuals who were infectious at  $t_{n-1}$  but are removed from  $I_n$  at  $t_n$ , because they are either in quarantine or because they recovered;
- $R_n$  be the number of so-called *removed* individuals; that is, people who are either immune or in quarantine at time  $t_n$ .

**Dynamics.** We now describe the dynamics of the pandemic system. By definition, the number of susceptible people satisfies  $S_n = N - I_n - R_n$ ;  $S_n$  represents the part of the population that can

be infected at time  $t_n$ . New infections are modeled in the following way. Any susceptible person at time  $t_{n-1}$  gets infected over  $[t_{n-1}, t_n)$  with probability

$$\beta_{n-1} \frac{I_{n-1}}{N}. \quad (2.1)$$

Here,  $\beta_{n-1}$  is the *infection* or *transmission rate*: it reflects the average number of social contacts of a susceptible person in  $[t_{n-1}, t_n)$  and the infectiousness of the virus (how likely a susceptible person gets infected when meeting an infected person). The fraction  $\frac{I_{n-1}}{N}$ , on the other hand, measures the probability of encountering an infectious person. Infection events are assumed to be independent across susceptible individuals. Since the quantity in formula (2.1) is usually small and  $S_{n-1}$  is large, we model the new infections  $I_n^+$  as a Poisson random variable with parameter  $\lambda_{n-1} = \beta_{n-1} \frac{I_{n-1}}{N} S_{n-1}$ , so that  $\lambda_{n-1}$  is the average number of new infections in the population over the time interval  $[t_{n-1}, t_n)$ .

Next, we consider the number of positive tests. An infectious person at time  $t_{n-1}$  is detected in the interval  $[t_{n-1}, t_n)$  with probability  $q \in [0, 1]$ . The parameter  $q$  accounts for the availability of tests and for the intensity of public screening programs. We assume, for simplicity, that tests are fully reliable; i.e. that a test is positive if and only if a tested person is infectious. We assume that tests occur independently across infected people. In that case, the conditional distribution of positive tests at time  $t_n$ , given the number  $I_{n-1}$  of infectious people at time  $t_{n-1}$ , is binomial with parameters  $I_{n-1}$  and  $q$ . A person who tests positively is immediately put in quarantine and hence removed from the pool of infectious people. Moreover, infectious people who are not detected move to the removed state upon recovery from the infection. Thus, at any time  $t_n$ , the number of infectious people is reduced by  $I_n^- = P_n + \gamma I_{n-1}$ , where  $\gamma > 0$  is the inverse of the average time a non-detected individual is infectious. Finally, we assume that a removed person loses immunity and becomes susceptible again with rate  $\delta$ , where  $1/\delta$  is the average time an infected person enjoys immunity. For instance,  $\delta \sim \frac{1}{200}$  says that people who recovered from the virus on average do not get infected again for about 200 days.

Summarizing, the dynamics of the system are as follows. For  $n \geq 1$ ,  $S_n = N - R_n - I_n$  and  $I_n = I_{n-1} + I_n^+ - I_n^-$ , where

$$\begin{cases} I_n^+ \sim \text{Poisson}(\beta_{n-1} \frac{I_{n-1}}{N} S_{n-1}), \\ I_n^- = P_n + \gamma I_{n-1} \text{ for } P_n \sim \text{Binomial}(\lfloor I_{n-1} \rfloor, q), \\ R_n = R_{n-1} + I_n^- - \delta R_{n-1}, \end{cases} \quad (2.2)$$

(here  $\lfloor \cdot \rfloor$  denotes the floor). These dynamics describe a compartmental model; that is, each individual, at a given time, is either susceptible, or infectious or removed.

We assume that the infection rate satisfies  $\beta_n = \exp(\Psi_n)$ , where  $\Psi_n$  is a first order autoregressive process with dynamics

$$\Psi_n = \Psi_{n-1} + \kappa(\mu - \Psi_{n-1}) + \sigma Z_n, \quad (2.3)$$

for  $n \geq 1$ , for a sequence of independent standard normal random variables  $\{Z_n\}_{n \geq 0}$  and parameters  $\kappa, \sigma > 0$  and  $\mu \in \mathbb{R}$  that will be estimated via particle filtering. Throughout, we assume an initial distribution of the system, that is the distribution of  $I_0$ ,  $R_0$  and  $\Psi_0$ . It is clear from (2.2) and (2.3) that the triple  $(I, R, \Psi)$  forms a discrete-time Markov chain.

There are several reasons for modelling the infection rate  $\beta$ , respectively its logarithm  $\Psi$ , by a process with mean-reverting behaviour. To begin with,  $\beta$  is closely related to the effective reproduction rate  $(\mathcal{R}_n)_{n \geq 0}$  (see below), and eyeballing the time series of estimates for  $\mathcal{R}_n$  provided by the Austrian health agency AGES (see Figure 7) strongly suggests mean-reverting dynamics. Moreover, mean-reversion is in line with the strategy pursued by many European governments who tightened policy measures when infection numbers were high (that is, after a period with high value of the index  $\mathcal{R}_n$ ) and who loosened measures after infection numbers had fallen to sustainable values.

**Observations.** The true number of infectious people is unknown, as this quantity includes asymptomatic infections or infected people that have not (yet) taken a test. Since infections are unobservable and random, we cannot observe the infection rate  $\beta_n$  (or equivalently its logarithm,  $\Psi_n$ ). At any time  $n \geq 1$ , the available information is thus provided by the number of positive tests  $P_n$ , whereas all other variables are latent. Formally, the available information can be described by the *information filtration*

$$\{\mathcal{F}_n\}_{n \geq 0}, \text{ where } \mathcal{F}_n = \sigma(P_j, 1 \leq j \leq n).$$

Partial information emerges very naturally in the context of Covid-19 and taking this feature into account is an important aspect of our contribution. Note also that other data sources, such as results from sewage screening or sentinel systems, are easily integrated into our approach (but this is left for future research).

**Reproduction rate.** The effective reproduction rate  $\mathcal{R}_n$  is a measure for the number of individuals that are on average infected by a given infectious person, given the state of the pandemic system at time  $t_n$ . This parameter plays a crucial role in the local dynamics of an epidemic; in particular, for  $\mathcal{R}_n > 1$  the number of infected people grows exponentially (for short time horizons), see for instance Diekmann et al. (2013). To identify  $\mathcal{R}_n$ , note first that an infected individual transmits the disease, on average, to  $\beta_n S_n / N$  people per day. Moreover, the time that elapses before an infected person transits to the removed state is the minimum of  $\tau^{\text{rec}}$  (the time up to recovery) and  $\tau^{\text{quar}}$  (the time until the person tests positively and is put into quarantine). Under our model dynamics,  $\tau^{\text{rec}}$  and  $\tau^{\text{quar}}$  have a geometric distribution with parameter  $\gamma$  and  $q$ , respectively. These stopping times are independent, so that  $\min\{\tau^{\text{rec}}, \tau^{\text{quar}}\}$  follows a geometric distribution with parameter  $\gamma + q - \gamma q \approx \gamma + q$ . Hence, the expected time up to removal satisfies  $\mathbb{E}(\min\{\tau^{\text{rec}}, \tau^{\text{quar}}\}) \approx (\gamma + q)^{-1}$ , and

$$\mathcal{R}_n \approx \frac{\beta_n S_n}{\gamma + q N}. \quad (2.4)$$

Since  $\beta_n$  and  $S_n$  are not observable in our setup, we consider the *estimated effective reproduction rate*  $\hat{\mathcal{R}}_n = \mathbb{E}[\mathcal{R}_n | \mathcal{F}_n]$  instead.

### 3. STATISTICAL METHODOLOGY

To address the problem of computing the posterior distribution of the state variables, as well as that of estimating model parameters, we use a nested particle filtering approach, suggested first by Crisan and Miguez (2018).

The general idea of this methodology is to perform two nested layer of filtering: the first layer involves parameters, and the second layer allows to compute the filtered state variables given a sample in the parameter space. To briefly explain this algorithm we let  $(X_n)_{n \geq 1}$  be the vector of state variables, which consists of  $(I_n, R_n, \Psi_n)_{n \geq 0}$ , and denote by  $\Theta = (\kappa, \sigma, \mu)$  the vector of parameters. We assume that the parameters  $q$ ,  $\gamma$  and  $\delta$  are derived from other data (e.g. medical data and other statistical studies), and hence represent a fixed input of our model.

In the initialisation step of the nested particle filtering procedure,  $K$  particles for the parameter vector are drawn from a prior distribution, say  $\mu_0$ , and, for each of these particles,  $M$  particles for the state vector are drawn from a distribution  $\pi_0$ <sup>1</sup>. At each recursion step (from  $n - 1$  to  $n$ ), the parameter particles are first agitated, or *jittered*, using a truncated Gaussian kernel with mean corresponding to the parameter estimates at the previous time point and variance  $\epsilon_\kappa$ ,  $\epsilon_\sigma$  and  $\epsilon_\mu$ , respectively, to restore particle diversity. In this way, all particles are subjected to a small perturbation. This step ensures a certain dispersion of the particle cloud and prevents the algorithm from shrinking towards a wrong value. Second, for each of these parameter sets, the state particles are propagated using model dynamics with new parameter values. Then, the likelihood of each particle is computed using the new information (i.e. the observed positive tests) and state particles are resampled with replacement as in a standard particle filter. Finally, parameter particles are resampled with replacement according to their weights, which gives an approximation to the posterior distribution of the parameters at time  $n$ . For a more detailed description of the algorithm, we refer to Crisan and Miguez (2018).

There are several advantages of using this approach: first, it allows to approximate the posterior distribution of both the state  $(X_n)_{n \geq 1}$  and the parameters  $\Theta$ , conditional on the observations  $(P_n)_{n \geq 0}$ ; second, it is recursive; third, it is known to converge under suitable assumptions, see again Crisan and Miguez (2018) for details.

In the sequel, we report our numerical analysis. We first apply the filtering algorithm on simulated data in Section 4. Then, we test it on real data from Austrian COVID-19 infections in Section 5.

#### 4. SIMULATION RESULTS

The goal of this section is to test the nested particle filtering on simulated data, using the model in Section 2. In this study, we have set initial values and the *true* parameters according to the values in Appendix A. We have also assumed that the probability of a positive test, the average duration of the illness and the average natural immunity period (i.e.  $q, 1/\gamma, 1/\delta$ ) are given (i.e. not estimated via filtering) and we fixed them consistently with the values reported by e.g. the Austrian Ministry of Health, see Richter et al. (2020). We have run the simulation for a period of  $T = 2$  years (731 days), which is roughly consistent with the length of the real data. In Figure 1, we represent a simulated trajectory of the (unobservable) state process  $(I_n)_n$  and the observation process  $(P_n)_n$  for  $n = 1, \dots, 731$ . These paths show qualitative properties that are similar to real Covid-19 infection data; for instance, our model naturally generates waves of infections. Notice that in the last months

---

<sup>1</sup>In the simulation study we assume that the prior distribution of the parameters is uniform between 1% and 500% of the true value, whereas in the data analysis we take uniform distribution on an interval of reasonable values. We also assume that  $I_0$  has Gamma distribution with parameters  $(0.2P_0/q, 0.2)$ ,  $R_0 = 0$ , and  $\Psi_0$  has Gaussian distribution with mean  $0.4 + \log(\gamma + q)$  and variance 0.175. See Appendix A for more details.

of the simulation period the number of positive tests is very low, which affects the estimates of the infection rate and the effective reproduction rate (see below).

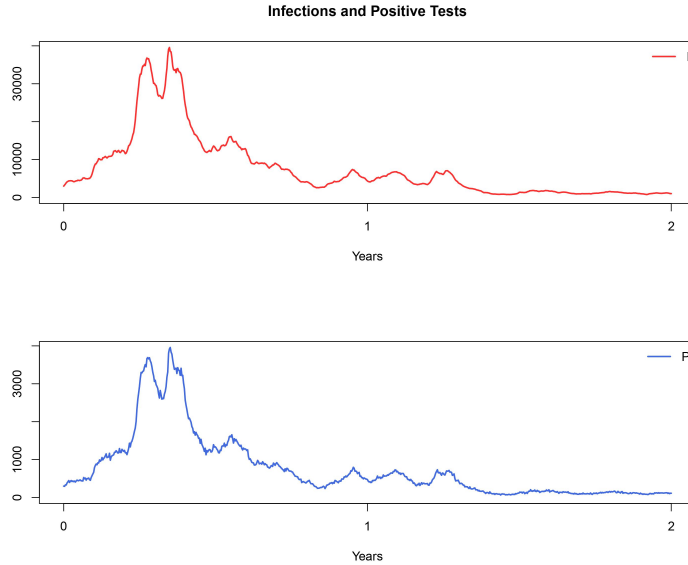


FIGURE 1. Simulated trajectory of the number of infectious people (state process) in the upper panel, and the number of positive tests (observation process) in the lower panel.

We have used the nested particle filtering described in Section 3 to estimate the number of infections, the infection rate  $(\beta_n)_n$ , the reproduction rate  $(\mathcal{R}_n)_n$  and the model parameters. The results discussed below have been averaged over 50 independent rounds.

Figure 2 reproduces the true trajectory (grey line) of the effective reproduction rate  $(\mathcal{R}_n)_n$  and the filtered trajectory (black line) from the observation of positive tests. This plot suggests that the true trajectory exhibits higher variance than the filtered one: indeed, in general the filter captures the trend of the signal process quite well, but is not able to detect small movements in short time. This is particularly evident toward the end of the simulation period, when the amount of information (i.e. the number of positive tests) is very small.

Next, we discuss the estimates of unknown parameters  $(\kappa, \sigma, \mu)$  (see the dynamics of  $\Psi_n = \log(\beta_n)$  in equation (2.3)). Posterior distributions are visualized in Figure 3. In each panel, the two blue lines correspond to 5% (bottom line) and 95% (top line) quantiles of the posterior distribution and the red line to its mean, while the black line corresponds to the true value of the parameter.

We immediately see that the estimate of  $\mu$  seems to be extremely accurate, while the values of  $\kappa$  and  $\sigma$  seem to be more difficult to estimate. This is particularly true for  $\kappa$ , whose estimate, for instance, is larger than the true one throughout the considered period. A slightly better estimate is obtained for the volatility  $\sigma$ . We have attributed the difficulty in identifying these parameters to a couple of reasons. First, we have relatively few observations, corresponding to two years. We decided to run our algorithm for two years only to be roughly consistent with the amount of data available for the Covid-19 pandemic. Second, the range for these values is relatively small.

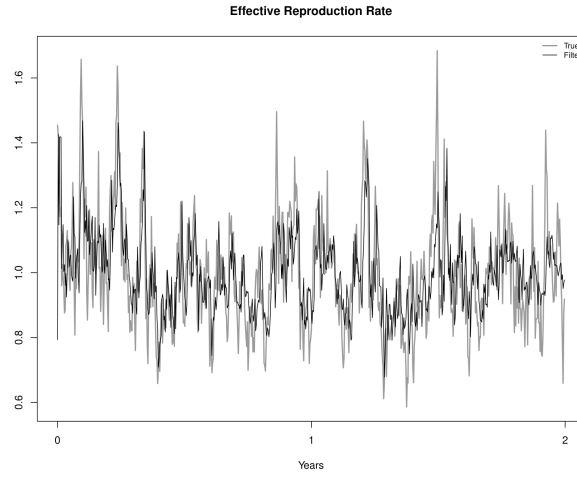


FIGURE 2. True (grey line) and filtered (black line) trajectory of the effective reproduction rate from simulated data

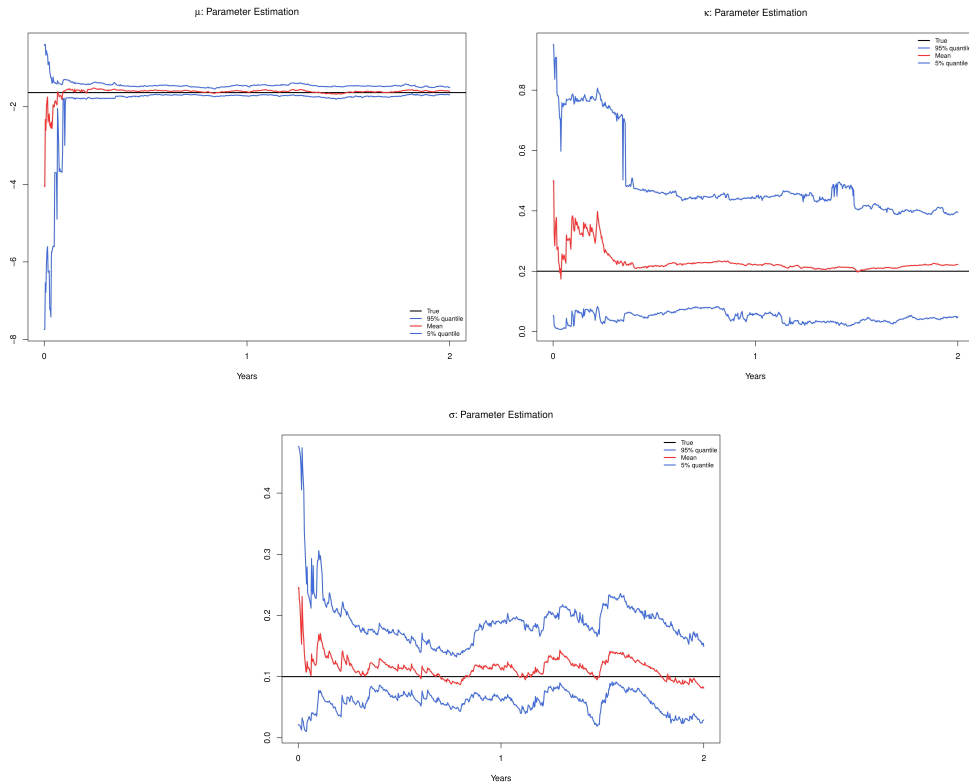


FIGURE 3. Filtered distribution of  $\mu$ ,  $\kappa$ , and  $\sigma$  from simulated data. Blue lines correspond to 5% and 95% quantiles, the red line to the mean and the black line is the true value.

Nevertheless, the algorithm is able to detect their magnitude quite rapidly. Moreover, higher values for  $\sigma^2$  and for  $\kappa$  tend to have an offsetting effect (recall that the long-run variance of  $\Psi_n$  is  $\sigma^2/2\kappa$ .)

The mean relative errors for  $\kappa$ ,  $\sigma$  and the ratio  $\sigma^2/2\kappa$  plotted in Figure 4 seem to confirm our considerations; in particular, the large relative errors of  $\kappa$  and  $\sigma$  counterbalance each other, leading to a better estimate for  $\sigma^2/2\kappa$ . We have also obtained a very small error for the parameter  $\mu$ , as expected.

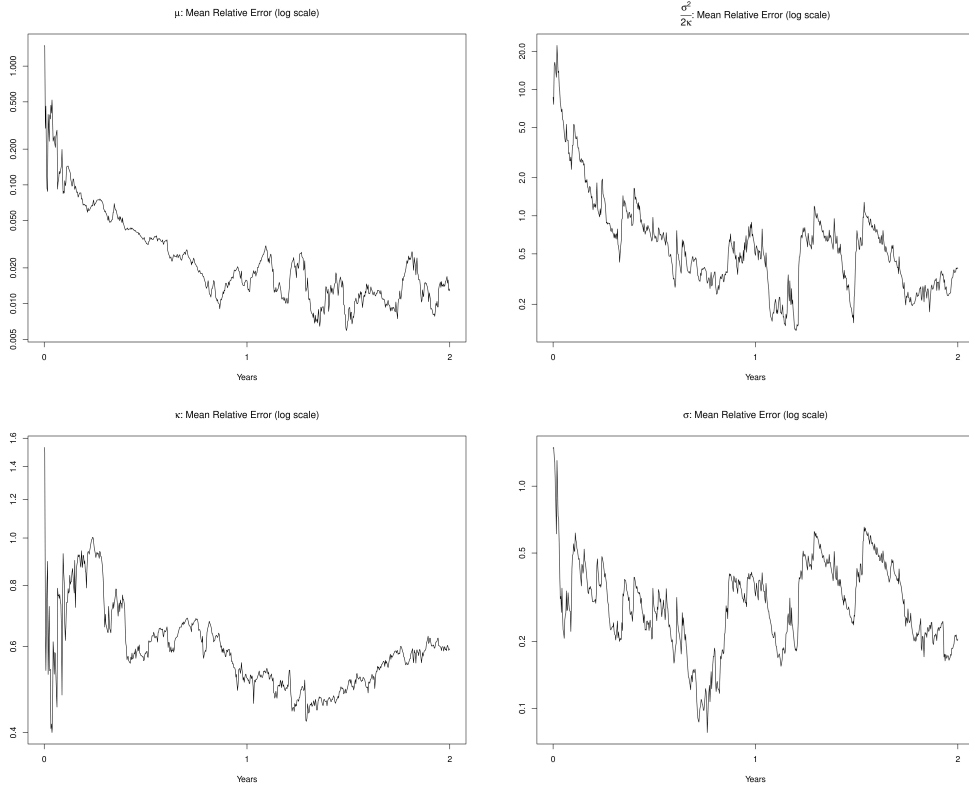


FIGURE 4. Mean relative errors for  $\mu$  (top left panel),  $\sigma^2/2\kappa$  (top right panel),  $\kappa$  (bottom left panel) and  $\sigma$  (bottom right panel), on a logarithmic scale.

Finally, we carried out robustness checks to ensure that small changes in the parameter  $q$  and  $\gamma$  do not affect our estimates too strongly, and we observed that the filtered effective reproduction rate corresponding to slightly varied values of these parameters presents very similar qualitative and quantitative characteristics.

## 5. EMPIRICAL RESULTS

In this section, we apply the nested particle filtering to Austrian Covid-19 data from May 1, 2020 to June 15, 2022. Figure 5 shows the positive tests in this period. In particular, we have used a 7-day rolling average of confirmed cases to avoid weekly seasonality effects, such as the fewer tests performed over the weekend. We have set the parameters of the model and of the particle filter according to the values in Appendix B.

We begin with the filtered estimate of the infection rate  $\beta$ , which is provided in Figure 6. Here, we observe an upward trend from the beginning of 2022. This is probably due to the arrival of

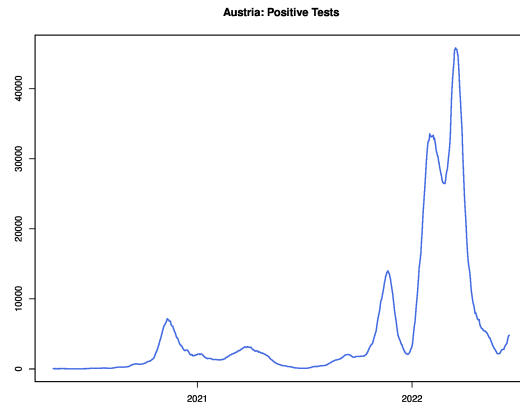


FIGURE 5. Confirmed cases of Covid-19 in Austria (1 May 2020 – 15 Jun 2022)

new and highly contagious virus variants (Delta and in particular Omicron), which has produced an increase in the number of cases.

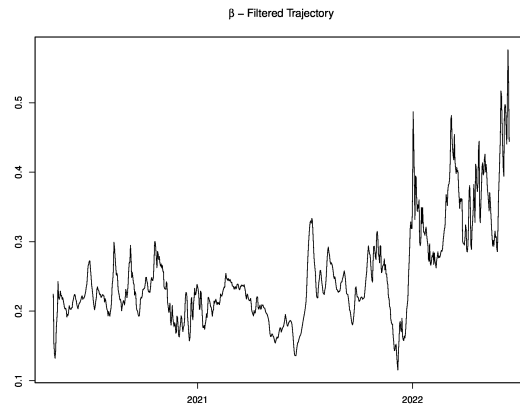


FIGURE 6. Estimates for the infection rate  $\beta$  from Austrian Covid-19 data (1 May 2020 – 15 Jun 2022).

Next, we focus on the effective reproduction rate ( $\mathcal{R}_n$ , see equation (2.4)). In Figure 7, we compare our filtered estimates (grey line) with the official estimate published by the Austrian health agency AGES (black line). The latter is computed using a simple Bayesian model with Gamma-distributed prior and Poisson observations, see Richter et al. (2020) for details. The plot shows that the qualitative behaviour of both estimates is very similar; however, our filtered estimate exhibits more variability and higher spikes, in particular starting from mid-2021. This seems to suggest that our filter reacts faster to changes. Notice that, while the infection rate  $\beta$  is persistently higher in the first half of 2022 (cf. Figure 6), the effective reproduction rate displays a spike at the beginning of 2022 and then immediately comes back to the usual values. This is due to the counterbalancing effect that a large part of the population got infected in a small time window (due to higher contagiousness of the virus variants), reducing substantially the number of susceptible individuals.

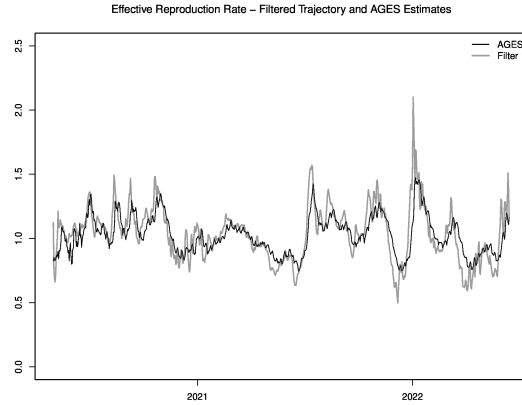


FIGURE 7. : Estimates for the effective reproduction rate from Austrian Covid-19 data (1 May 2020 – 15 Jun 2022): in grey the filtered estimate of  $\mathcal{R}_n$  using our methodology; in black the estimate published by the Austrian health agency AGES.

Figure 8 shows the evolution, over time, of the posterior distribution of the unknown parameters  $\kappa$ ,  $\sigma$  and  $\mu$ . As expected, we immediately observe quite good convergence for the parameter  $\mu$ , but estimates seem to narrow down to some specific value in  $\kappa$  and  $\sigma$  as well. A promising result is the fact that, after an initial short period, the particle filter quickly identifies a range of plausible values for these parameters. We also observe that, from the beginning of the second year of data, the distribution of  $\kappa$  seems to shrink toward a value that is smaller than in the first year of data; moreover  $\mu$  tends to be larger. This effect does not seem to be due to learning, and it may suggest that parameters are, in fact, time-varying (in particular, the arrival of Omicron might have started a new regime). However, we need to be careful with such conclusions, since we saw in the simulation study that  $\kappa$  and  $\sigma$  are difficult to estimate, and since we ran the filtering algorithm under the assumption of constant parameters. One possible way to confirm our conjecture is to split the data, and try to get an estimate of the parameters in those periods that may correspond to different regimes; however, this is not really feasible with the relatively short series of observations available to date.

## 6. FORECASTING AND MODEL TESTS

A key application of an epidemiological model is to make forecasts regarding the development of infection numbers, which are used to gauge potential stress for the health system and which serve as a basis for decisions on containment measures. Moreover, analyzing the quality of model-based predictions is a natural way of testing a given model. Therefore, in this section, we discuss forecasts and model tests for our setup. Here we draw on ideas developed in the context of backtesting statistical models in financial risk management, see for instance McNeil et al. (2015).

**6.1. Methodology.** The key quantity for forecasting and testing is the *predictive distribution* of future positive tests over a time horizon  $\Delta$ , with distribution function

$$F_{n,\Delta}(x) = \mathbb{P}(P_{n+\Delta} \leq x \mid \mathcal{F}_n).$$

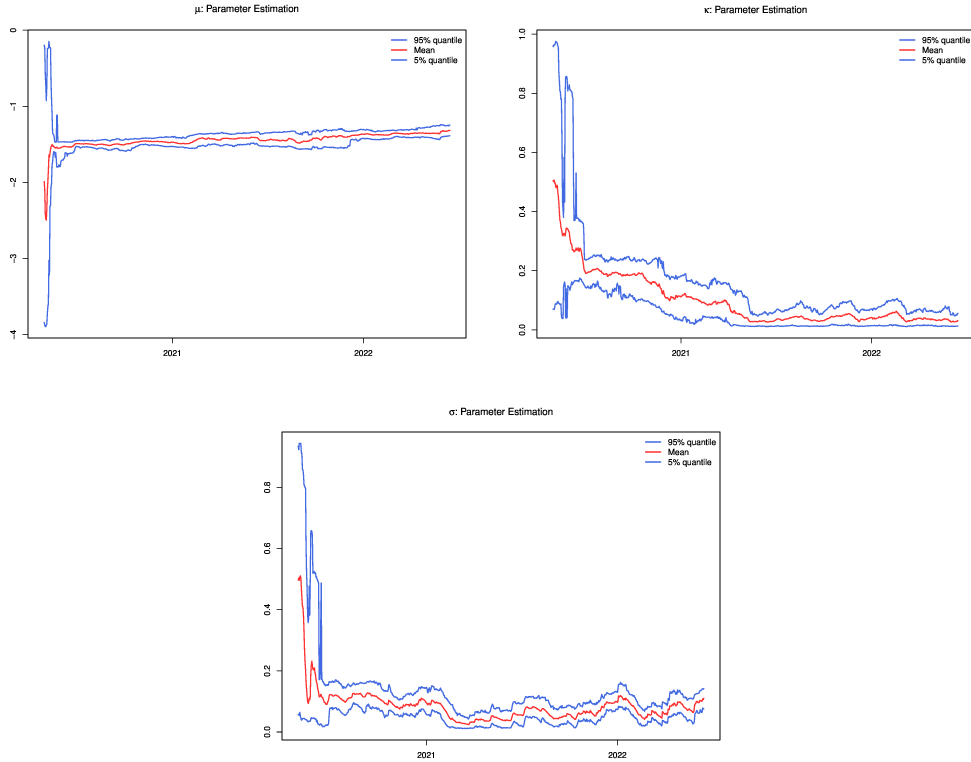


FIGURE 8. Filtered estimates of the parameters  $\mu$ ,  $\kappa$ , and  $\sigma$  for the Austrian infection data.

To compute an estimate  $\widehat{F}_{n,\Delta}$  of  $F_{n,\Delta}$ , we rely on simulations: we first run the particle filter over the period  $[0, t_n]$ , which provides an approximation of the conditional distribution of the state variables and the model parameters given  $\mathcal{F}_n$ . We then draw realisations of  $I_n, R_n, \psi_n$  and of the parameters  $\mu, \kappa, \sigma$  from that distribution, which we use to generate trajectories of  $I, R, \psi$  and  $P$  over the horizon  $t_n, \dots, t_n + \Delta$  using the dynamics (2.2) and (2.3).

There are various ways to generate *point forecasts* from the predictive distribution. It is natural to use elicitable forecasts, (forecasts minimizing a suitable scoring function) such as the median, higher quantiles or the mean. Now, in our setup the predictive distribution is skewed with a very heavy upper tail (see next paragraph), and the mean yields quite unstable forecasts. This suggests to use quantile based forecasts such as the median. In fact, underestimating future infection numbers has typically more adverse consequences than overestimating them, so that one might resort to higher quantiles such as the 75% quantile instead.

Formal *statistical tests* of our methodology can be based on the following classical result of Rosenblatt (1952). Fix some horizon  $\Delta$  and consider non-overlapping prediction dates  $t_{n_1}, t_{n_2} = t_{n_1} + \Delta, \dots, t_{n_m} = t_{n_1} + m\Delta$ . Suppose, moreover, that the predictive distribution is correctly specified, that is  $\widehat{F}_{n_j,\Delta} = F_{n_j,\Delta}$  for all  $j$  (this is the null hypothesis for our model test). Then,

the random variables  $\widehat{U}_j := \widehat{F}_{n_j}(P_{n_j+\Delta})$ ,  $1 \leq j \leq m$ , are independent and identically distributed standard uniform.<sup>2</sup>

This result is the basis for a multitude of statistical tests; see for instance Gordy and McNeil (2020). Simple tests use *quantile exceedances*. Fix  $\alpha \in [0, 1]$ . Then the quantile exceedances

$$I_{n_j}^\alpha = 1_{\{P_{n_j+\Delta} > q_\alpha(\widehat{F}_{n_j,\Delta})\}}, \quad 1 \leq j \leq m,$$

are independent and identically Bernoulli-distributed with  $p = 1 - \alpha$ , so that the number of exceedances  $M^\alpha = \sum_{j=1}^m I_{n_j}^\alpha$  has a binomial distribution with parameters  $m$  and  $p = 1 - \alpha$ . This can be tested with a simple binomial test. More generally, one may test the several quantile exceedances jointly by means of *multinomial tests* as explained below (see, also Kratz et al. (2018)). Fix quantile levels  $0 = \alpha_0 < \alpha_1 < \dots < \alpha_l < \alpha_{k+1} = 1$  and, for  $0 \leq l \leq k$ , denote by

$$M^{[\alpha_l, \alpha_{l+1}]} = \sum_{j=1}^m 1_{\{q_{\alpha_j}(\widehat{F}_{n_j,\Delta}) \leq P_{n_j+\Delta} < q_{\alpha_{j+1}}(\widehat{F}_{n_j,\Delta})\}}$$

the number of visits of  $\{\widehat{U}_{n_j}, 1 \leq j \leq m\}$  to the cell  $[\alpha_l, \alpha_{l+1})$ . It follows that the  $k + 1$  rvs  $M^{[\alpha_l, \alpha_{l+1}]}$ ,  $0 \leq l \leq k$ , have a *multinomial* distribution with  $k + 1$  cell probabilities  $p_1 = \alpha_1$ ,  $p_2 = \alpha_2 - \alpha_1, \dots, p_{k+1} = 1 - \alpha_k$ . This can be tested with goodness of fit tests such as the exact multinomial test, see Menzel (2021).

**6.2. Empirical results.** We now apply these ideas to the Austrian Covid-19 data. We consider horizons up to 14 days, as this is a common forecasting horizon. The parameters of the model and of the particle filter are given in Appendix B.

*Predictive distribution.* In Figure 9, we plot several quantiles of  $\widehat{F}_{n,\Delta}$  for  $\Delta = 1, 2, \dots, 14$  together with the actually observed positive tests for two different prediction dates  $t_n$ . The left plot shows the forecasts made on December 23, 2021 – that is, shortly before the start of the Omicron wave in Austria, while the right plot shows the forecasts from January 20, 2022. We use a logarithmic scale for the quantiles, since the predictive distribution is very skewed. The strong skewness of the predictive distribution can also be seen from Table 1, where we report numerical values of various quantiles and of the mean of  $\widehat{F}_{n_j,14}$  for these two prediction dates.

Looking at the left plot, we see that the model predicts the decline of the Delta wave well, but the high infection numbers caused by the onset of Omicron are close to the 90% quantile of the predictive distribution. This is to be expected: since our model is informed only by observations of past positive tests it does not “know” about the emergence of a new virus variant. Such information would need to be entered manually by the epidemiologist, for instance by an upward shift in the distribution of the infection rate at  $t_n$ . The right plot shows that, by January 20, 2022, the model has learned the different regime and actual cases are between the median and the 75% quantile of  $\widehat{F}_{n,\Delta}$ . However, even on December 20, the infection numbers of the Omicron wave are below

---

<sup>2</sup>Strictly speaking this is true only if  $\widehat{F}_{n,\Delta}$  is continuous. In our setup  $P_n$  is conditionally binomial and  $\widehat{F}_{n,\Delta}$  is computed by simulation, therefore it is discrete. However, the number of simulations used is be large and the conditional distribution of  $P_n$  is very well approximated by a normal, so that under the null the distribution of  $\widehat{F}_{n,\Delta}(P_{n+\Delta})$  is very close to a standard uniform distribution.

prediction date	10%	25%	50%	75%	90%	95%	mean
Dec 23,2021	494	851	1411	3509	16338	79142	20194
Jan 20,2022	8388	13372	24845	46603	155557	248978	56468

TABLE 1. Quantiles and mean of the predictive distribution  $\widehat{F}_{n,14}$  for two different prediction dates and a horizon of 14 days. Note that the distribution is very skewed with high upper quantiles and a mean exceeding the the 90% quantile (for Dec 23, 2022) respectively the 75% quantile (for Jan 20, 2022)

the 90% quantile of the predictive distribution, and thus well within the range of possible future scenarios generated by our model.

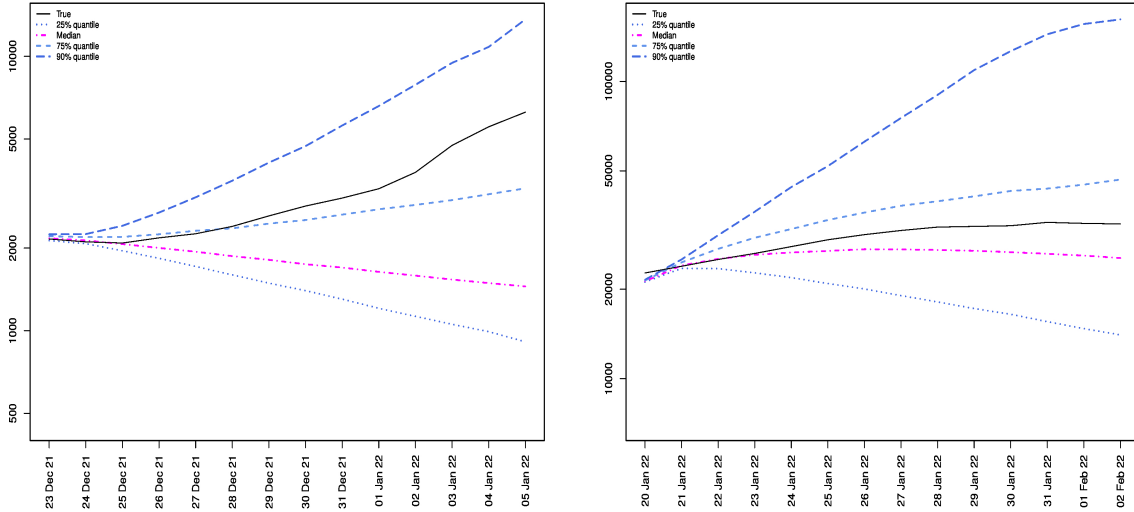


FIGURE 9. Left: quantiles  $q_\alpha(\widehat{F}_{n,\Delta})$ ,  $\alpha = 0.25, 0.5, 0.75, 0.9$ , of  $\widehat{F}_{n,\Delta}$  for the prediction date  $t_n = 23/12/2021$  and prediction horizon  $\Delta$  between one and 14 days together with the actually observed positive tests; right quantiles and mean of of  $\widehat{F}_{n,\Delta}$  and realized positive tests for  $t_n = 20/01/2022$ .

*Formal tests.* For our tests, we use a horizon of  $\Delta = 14$ . Since the particle filter takes some time to start converging, we chose September 1, 2021, as the date of the first test, which yields  $m = 20$  non-overlapping testing dates. We consider the quantile levels  $\alpha_1 = 0.25$ ,  $\alpha_2 = 0.5$ ,  $\alpha_3 = 0.75$ ,  $\alpha_4 = 0.9$  in our tests. In Table 6.2, we tabulate the expected and the observed number of quantile exceedances and cell visits. We see that the quantile exceedances are quite close to their expected value, and a binomial test applied to the observed quantile exceedances yielded a high  $p$ -values (details are omitted). We finally ran the exact multinomial test for cell visits and obtained a  $p$ -value of 0.521. These convincing test results support the methodology proposed in this paper. Note, however, that the precise outcome of numerical tests varies somewhat with the chosen quantile levels, testing horizon and testing dates. Moreover, the estimated predictive distribution  $\widehat{F}_{n,\Delta}$  is sensitive to the

$\alpha$	0.25	0.5	0.75	0.9	cell	< 0.25	0.25–0.5	0.5–0.75	0.75–0.9	>0.9
exp.	15	10	5	2	exp.	5	5	5	3	2
obs.	15	11	4	0	obs.	5	4	7	4	0

TABLE 2. Left: expected and observed quantile exceedances; right: expected and observed cell visits.

choice of settings in the nested particle filter, and some experimentation is necessary (especially given the relatively short series of observations).

#### APPENDIX A. INPUTS FOR THE SIMULATION STUDY

Simulation parameters (true values) and other inputs.

- $q = 10\%$
- $\gamma = 1/10$
- $\delta = 1/200 = 0.05$
- $\kappa = 0.2$
- $\sigma = 0.1$
- $\mu = \log(\gamma + q) + \frac{\sigma^2}{2\kappa} \approx -1.63$
- Number of individuals:  $N = 8.917 \cdot 10^6$
- Number of confirmed cases at time 0:  $P_0 = 300$
- Number of days:  $N^{days} = 731$  (including time 0)
- Time step:  $\Delta = t_n - t_{n-1} = 1$  day

Settings for the nested particle filtering.

- Prior for  $\Psi$ : normal with mean  $\log(\gamma + q) - \sigma^2/2\kappa \approx -1.63$  and standard deviation 0.175
- Prior for  $I_0$ : gamma with shape  $0.2P_0/q =$  and rate 0.2
- Prior for  $\kappa$ ,  $\sigma$  and  $\mu$ : uniform over 1% and 500% of true values
- Number of particles in the state space  $M = 500$  and in the parameter space  $K = 500$
- Variance of the jittering kernels  $\epsilon_\kappa = \epsilon_\mu = \epsilon_\mu = 5M^{-2}$

#### APPENDIX B. INPUTS FOR THE REAL DATA ANALYSIS

Data characteristics.

- Time period: from May 1, 2020, to June 15, 2022
- Total number of individuals:  $N = 9.028 \cdot 10^6$  (i.e. population of Austria)
- Observations  $P$ : 7-day rolling average of confirmed cases
- $P_0 = 47$  (number of confirmed cases, i.e. value of 7-day rolling average at the starting date)

Fixed parameters and other inputs.

- $q = 10\%$
- $\gamma = 1/10$
- $\delta = 1/200 = 0.05$

- Number of days:  $N^{days} = 776$  (including time 0)
- Time step:  $\Delta = t_n - t_{n-1} = 1$  day

Settings for the Nested Particle Filtering.

- Prior for  $\Psi$ : normal with mean  $\log(\gamma + q)$  and standard deviation 0.1
- Prior for  $I_0$ : gamma with shape  $0.2P_0/q = 0.2 \cdot 470$  and rate 0.2
- Prior for  $\kappa$ : uniform over  $[0.01, 1]$
- Prior for  $\sigma$ : uniform over  $[0.01, 1]$
- Prior for  $\mu$ : uniform over  $[-4, -0.01]$
- Number of particles in the state space  $M = 600$  and in the parameter space  $K = 600$
- Variance of the jittering kernels  $\epsilon_\kappa = \epsilon_\mu = \epsilon_\mu = 5M^{-2}$

## REFERENCES

- E. Alòs, M. E. Mancino, R. Merino, and S. Sanfelici. A fractional model for the COVID-19 pandemic: Application to Italian data. *Stochastic Analysis and Applications*, 39(5):842–860, 2021.
- A. Budhiraja, L. Chen, and C. Lee. A survey of numerical methods for nonlinear filtering problems. *Physica D: Nonlinear Phenomena*, 230(1-2):27–36, 2007.
- D. Crisan and J. Miguez. Nested particle filters for online parameter estimation in discrete-time state space Markov models. *Bernoulli*, 24:3039–3086, 2018.
- O. Diekmann, H. Heesterbeek, and T. Britton. *Mathematical tools for understanding infectious disease dynamics*, volume 7. Princeton University Press, 2013.
- M. Gordy and A. McNeil. Spectral backtests of forecast distributions with application to risk management. *Journal of Banking and Finance*, 116, 2020.
- A. Hasan, H. Susanto, V. Tjahjono, R. Kusdiantara, E. Putri, N. Nuraini, and P. Hadisoemarto. A new estimation method for COVID-19 time-varying reproduction number using active cases. *Scientific Reports*, 12(1):1–9, 2022.
- E.L. Ionides, D. Nguyen, Y. Atchadé, S. Stoev, and A.A. King. Inference for dynamic and latent variable models via iterated, perturbed bayes maps. *Proceedings of the National Academy of Sciences*, 112(3):719–724, 2015.
- M. Kratz, Y. Lok, and A. McNeil. Multinomial VaR backtests. *Journal of Banking and Finance*, 88:393–407, 2018.
- A. J. McNeil, R. Frey, and P. Embrechts. *Quantitative Risk Management: Concepts, Techniques and Tools*. Princeton University Press, Princeton, 2nd edition, 2015.
- U. Menzel. *EMT: Exact Multinomial Test: Goodness-of-Fit Test for Discrete Multivariate Data*, 2021. URL <https://CRAN.R-project.org/package=EMT>. R package version 1.2.
- L. Richter, D. Schmidt, and E. Stadlober. Methodenbeschreibung für die Schätzung von epidemiologischen Parametern des COVID 19 Ausbruchs österreich. Working paper, AGES, available from <https://www.ages.at/>, 2020.
- M. Rosenblatt. Remarks on a multivariate transformation. *The Annals of Mathematical Statistics*, 23(3):470–472, 1952.
- B. Stocks, T. Britton, and M. Höhle. Model selection and parameter estimation for dynamic models via iterated filtering: application to the Rotavirus in Germany. *Biostatistics*, 21:400–416, 2020.

L. Sun, C. Lee, and J. A. Hoeting. Parameter inference and model selection in deterministic and stochastic dynamical models via approximate Bayesian computation: modeling a wildlife epidemic. *Environmetrics*, 26(7):451–462, 2015.